ELSEVIER

Materials Science and Engineering A318 (2001) 197–210

MATERIALS SCIENCE & ENGINEERING A

www.elsevier.com/locate/msea

Effect of tempering temperatures on the mechanical properties and microstructures of HSLA-100 type copper-bearing steels

S.K. Dhua [a] *, Amitava Ray [a], D.S. Sarma [b]

[a] *Research and Development Centre for Iron and Steel, Steel Authority of India Ltd., Ranchi 834002, India*
[b] *Department of Metallurgical Engineering, Banaras Hindu University, Varanasi 221005, India*

Received 14 June 2000; received in revised form 23 February 2001

Abstract

Two copper-bearing high-strength low-alloy (HSLA) steels with chemistry similar to HSLA-100, were made on a laboratory scale, one in an air induction (100 kg) furnace and the other in a vacuum induction (50 kg) furnace. The ingots cast were hot-rolled to 25 mm thick plates which were subsequently austenitized and tempered at different temperatures (400–700°C) for 1 h. Evaluation of mechanical properties and microstructure of as-quenched and tempered plates revealed that substantial improvement in strength (YS-1024 and 1025 MPa; UTS-1079 and 1111 MPa for steels 1 and 2) occurred at the expense of impact toughness on tempering at 500°C owing to profuse Cu precipitation in the matrix. With increase in tempering temperature however, the notch toughness improved considerably, reaching peak values of 53 and 123 Joules (J) at −85°C for steels 1 and 2 at 650 and 700°C tempering temperatures, respectively. The partially recovered matrix and the coarsened Cu precipitates in this temperature range presumably enhanced dislocation movement and notch toughness.

Keywords: HSLA-100; Copper-bearing steels; Cu precipitation

1. Introduction

Quenched and tempered medium-carbon low-alloy steels are traditionally used for engineering structures demanding high strength and toughness. Although carbon is the prime element used for enhancing strength in these steels, it nonetheless is known to reduce weldability and impact toughness if present above a certain quantity [1]. Owing to the presence of 0.18–0.20 weight (wt.)% carbon and a high carbon equivalent of 0.8–0.9, the commonly used HY-80 and HY-100 grades of steels present difficulties in welding [1–5]. In order to overcome this problem, a new generation of low-carbon, copper-bearing HSLA steels have been developed [2–5]. In general, copper is perceived to be an undesirable element in steel owing to its associated hot-shortness problem. However, its judicious usage can improve the hardenability and atmoshpheric corrosion resistance of structural steels. Copper, by virtue of ε-copper precipitation, improves the strength in the HSLA class of steels without adversely affecting weldability. In the evolution of a new series of such alloys, the ASTM A 710 steel, with a composition (in wt.%) of 0.07 C, 1 Cu, 0.8 Ni, 0.7 Cr, 0.2 Mo and 0.04 Nb was the first to be developed [6–10]. Based on this composition, the HSLA-80 steel with a minimum yield strength (YS) of 552 MPa was developed in the 1980s for construction of hulls for naval ships and submarines [2,11]. The carbon level in this steel was kept below 0.08 wt.% as it was established that weldability was not adversely affected even at a higher carbon equivalent if the carbon content was restricted to <0.1 wt.% [1].

Although the HSLA-80 steel was certified by U.S. Navy for naval applications, its limitation of YS (552 MPa, maximum) made it unsuitable for use in structures subjected to complex dynamic loading, as commonly encountered in many important components of naval ships and submarines [2]. Moreover, because of its limited hardenability, the HSLA-80 steel is not

* Corresponding author. Fax: +91-651-501327.
E-mail addresses: aray@rdcis.bih.nic.in (A. Ray), dssarma@banaras.ernet.in (D.S. Sarma).

0921-5093/01/$ - see front matter
PII: S0921-5093(01)01259-X

Table 1
Chemical analysis of the experimental steels (wt.%)

Steel	C	Mn	Si	P	S	Cu	Cr	Mo	Ni	Nb	Al
1	0.026	0.62	0.11	0.014	0.013	1.73	0.58	0.68	3.37	0.03	0.004
2	0.03	0.73	0.29	0.017	0.016	1.52	0.75	0.70	3.12	0.03	0.038

considered suitable for making higher thickness plates [4]. The limitations of the HSLA-80 steel led to the development of HSLA-100 steel with higher strength (YS: 690 MPa), superior toughness and weldability. This steel contains higher amounts of Ni, Cu, Mn and Mo than those of earlier grades [12–18].

We had earlier investigated the structure–property relationships of an industrially made HSLA-100 steel which was processed through vacuum degassing route and hot-rolled to 51 mm thick plates [19]. In the present work, two experimental Cu-bearing HSLA steels with similar chemistry, but processed through air and vacuum induction furnace routes, were investigated. While the different steel making routes governed the characteristics of non-metallic inclusions (NMI), the microstructure of plates was influenced by down-stream rolling and heat-treatment regimes. The paper elucidates the effect of NMI characteristics and tempering temperatures on the microstructure and mechanical properties of heat-treated steel plates.

2. Experimental

Two experimental heats were made, one in a 100 kg capacity air–induction furnace and another in a 50 kg capacity vacuum-induction furnace. The air-induction furnace heat (steel $\neq 1$) was cast into $300 \times 100 \times 100$ mm size ingots, whereas the vacuum-induction furnace heat (steel $\neq 2$) was cast into ingots of 100 mm diameter and 400 mm length. The chemical analyses of the two steels are shown in Table 1.

The ingots were soaked at 1250°C for 2 h and hot-rolled into 25 mm thick plates in a 2-high experimental rolling mill. After hot-rolling, the plates were cooled in air. The as-rolled plates were cut in the longitudinal-through thickness (LT) orientation into 14 mm thick Charpy and tensile test blocks of suitable dimensions. For ensuring uniformity of sample location, test blocks were cut from a distance of 2–3 mm from the top/bottom surfaces. These test blocks were austenitized at 950°C for 40 min, quenched in water and subsequently tempered at different temperatures ranging from 400–700°C for 1 h, followed by quenching in water. All the aforesaid heat treatments were carried out in a salt bath furnace.

Microstructural examination of water-quenched as well as tempered steel plates were conducted in a 'NEOPHOT-30' model metallurgical microscope. For characterizing non-metallic inclusions, polished and unetched specimens were used, while microstructural studies were carried out on 2% nital-etched specimens. Quantitative image analysis of polished specimens was carried out in a LEICA make, 'Q-600' model image analysis system to quantify inclusion contents. The volume fractions of NMI present in each specimen were determined by scanning around 300 fields and the average value was reported (Table 2). Qualitative electron-probe microanalysis was carried out in a JEOL make, 'JCXA-733' model electron-probe microanalyser (EPMA) to ascertain inclusion chemistry. For precise identification of phases, X-ray diffractometric studies were also carried out on specimens using Mo target in a SIEMENS make, 'D-500' model X-ray diffractometer.

Thin foils for transmission electron microscopy were prepared in a twin-jet electropolisher using an electrolytic solution of 95% glacial acetic acid and 5% perchloric acid. These foils were examined in a JEOL 'JEM-4000 EX' transmission electron microscope (TEM) at 200 keV to observe the microstructural details.

Hardness measurements were conducted in a Vicker's hardness tester under 30 kg applied load and the average hardness of a particular sample was reported from measurements over 10 locations. Tensile testing was carried out on 6.25 mm diameter specimens in a 10 ton capacity 'INSTRON-1195' model universal testing machine, using a 25 mm gauge length (GL) extensometer. The tests were conducted in accordance with ASTM A 370 specification. Three specimens were tested for each heat-treatment condition and the average values were reported. Charpy impact tests were conducted using standard V-notch (2 mm deep notch) specimens ($10 \times 10 \times 55$ mm size) as per ASTM E 23 specification. The tests were conducted both at ambient (25°C) and subzero (-20 and -85°C) temperatures. The Charpy test

Table 2
Volume fraction of non-metallic inclusions in the experimental steels

Steel	Inclusion volume fraction (%)		
	Minimum	Maximum	Average
1	0.166	0.235	0.20
2	0.084	0.103	0.09

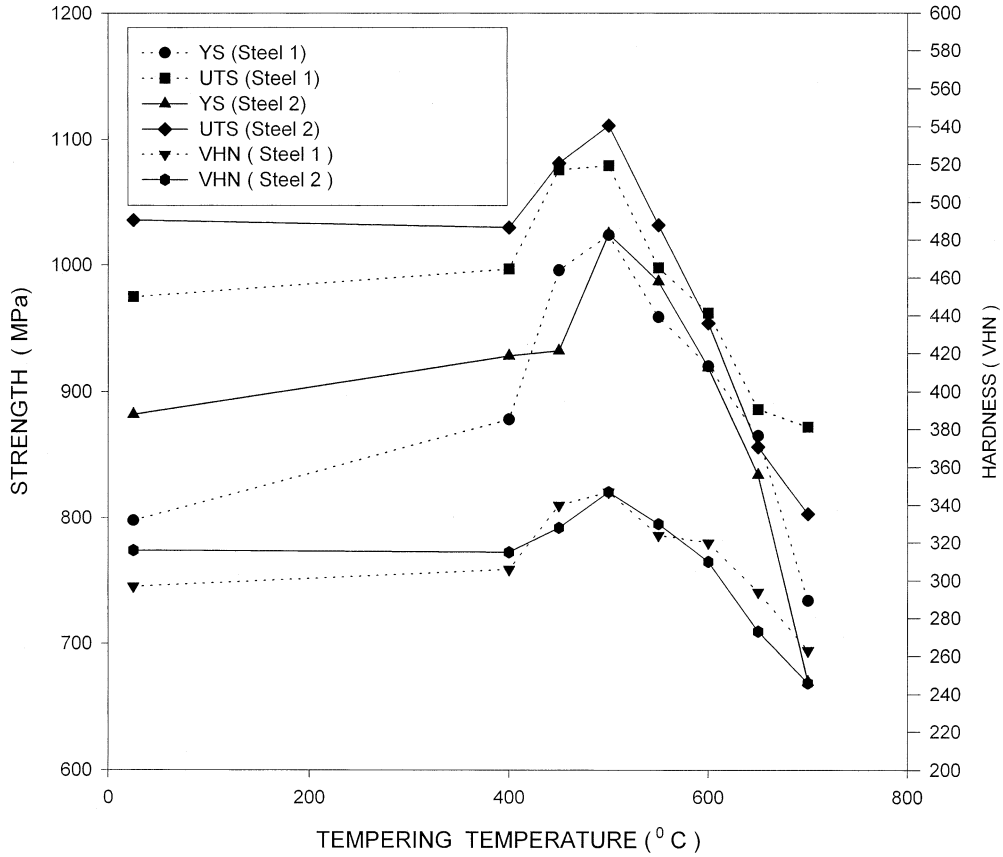

Fig. 1. Variation of Yield strength, ultimate tensile strength and hardness of steels 1 and 2 with tempering temperature.

specimens for the aforesaid tests were prepared in L–T orientation and notched transverse to the plate thickness. The broken Charpy specimens were examined in a JEOL make, 'JSM-840A' model scanning electron microscope (SEM) at an accelerating voltage of 20 keV to study fracture topography.

3. Results

3.1. Mechanical properties

3.1.1. Hardness

The average Vickers hardness values (VHN) of water-quenched plates of steels 1 and 2 were found to be 297 and 316 VHN, respectively. The corresponding hardness values decreased to 263 and 246 VHN upon tempering at 700°C. For both the steels, peak hardness value of 347 VHN was achieved after tempering at 500°C. The hardness versus tempering temperature plots of steels 1 and 2 are shown in Fig. 1.

3.1.2. Yield and tensile strength

In water-quenched and tempered condition, the YS was found to vary between 734–1024 and 670–1025 MPa for steels 1 and 2, respectively. The YS was found to be maximum at 500°C and minimum at 700°C within the experimental tempering range. The variation of YS and hardness with tempering temperature in both the steels are graphically shown in Fig. 1.

The ultimate tensile strength (UTS) of water-quenched and tempered plates varied between 872–1079 and 803–1111 MPa in steels 1 and 2, respectively. In both steels 1 and 2, peak UTS, similar to peak YS, was achieved after tempering at 500°C, while the minimum UTS was obtained at 700°C. Fig. 1 also depicts the variation of UTS with tempering temperature of steels 1 and 2 along with hardness and YS plots.

3.1.3. Elongation and reduction-in-area

The elongation (EL) percent of water-quenched and tempered plates varied between 15–22 and 16–25% for steels 1 and 2, respectively. The elongation was maximum for both the steels after tempering at 650°C and minimum in the water-quenched state. Fig. 2 shows typical elongation versus tempering temperature plots of both the steels.

The reduction-in-area (RA) percent of water-quenched and tempered plates varied between 60–69 and 65–75%, respectively for steels 1 and 2. The % RA was found to be maximum after tempering at 650°C for steel 1, whereas for steel 2, it was maximum after 700°C

tempering. The minimum values of % RA were attained in both the steels after tempering at 450°C. The variation of % RA with tempering temperature in steels 1 and 2 are shown in Fig. 2.

3.1.4. Charpy impact toughness

The Charpy V-notch (CVN) impact energy values of the water-quenched and tempered plates of steel 1 varied between 35–98 J at 25°C, 22–93 J at −20°C, and 7–53 J at −85°C. In case of steel 2 plates, the CVN energy values at the corresponding temperatures varied between 31–136, 26–130 and 9–123 J, respectively. In case of steel 1, the CVN energy was maximum after tempering at 650°C, whereas for steel 2, it was highest after 700°C tempering. Interestingly, the minimum CVN energy values were obtained for both the steels after 450°C tempering. The CVN energy versus tempering temperature plots of steels 1 and 2 tested at various test temperatures are shown in Fig. 3(a, b), respectively.

3.2. Microstructures

3.2.1. Optical microscopy

In unetched condition, NMI in water-quenched steel 1 were found to be mostly oxysulphide stringers (Fig. 4a). EPMA analysis confirmed that these stringers were essentially complexes of MnS and Al_2O_3–SiO_2. Few small size globular oxides and lenticular sulphides were also observed in this steel. Steel 2 on the other hand, mostly revealed small globular oxide inclusions (Fig. 4b) whose EPMA analysis confirmed presence of Fe and Si. In this steel, few stringers of oxysulphide inclusions were also observed.

The microstructures of steel 1 in water-quenched condition as well as after tempering at 700°C are shown in Fig. 5(a, b), respectively. The microstructure appears to be of lath martensite in the as-quenched condition and shows no significant difference after tempering at 700°C.

3.2.2. Transmission electron microscopy

TEM studies of the as-quenched steels revealed mixed microstructure of lath martensite and bainitic ferrite. A typical bainitic ferrite microstructure observed in steel 1 is shown in Fig. 6(a). Fig. 6 (b–c) show bright-field (BF) and dark-field (DF) micrographs of the same steel from different martensitic regions. The martensite laths were found to be associated with traces of retained austenite at lath boundaries, while very fine precipitates (approximately 10–25 nm diameter) of Cu and Nb(C,N) were also observed within the laths. The presence of retained austenite and the precipitates were confirmed by indexed selected area diffraction (SAD) patterns and are shown in Fig. 6(d–g), respectively.

The BF micrograph in Fig. 7 (a) shows typical unrecovered lath martensite structures observed in the steels tempered at 500°C. Profuse precipitation of Cu within the laths could be noticed in the BF and DF micrographs shown in Fig. 7 (b–c) which pertain to the same area. The SAD pattern of the precipitates and the corresponding index photograph are shown in Fig. 7 (d–e), respectively. The Cu precipitates observed were around 15–30 nm in diameter and were almost spherical in shape at this tempering temperature.

Transmission electron microscopy of the steels after tempering at 650°C showed partially recovered matrix with uniformly distributed Cu precipitates. Fig. 8 (a)

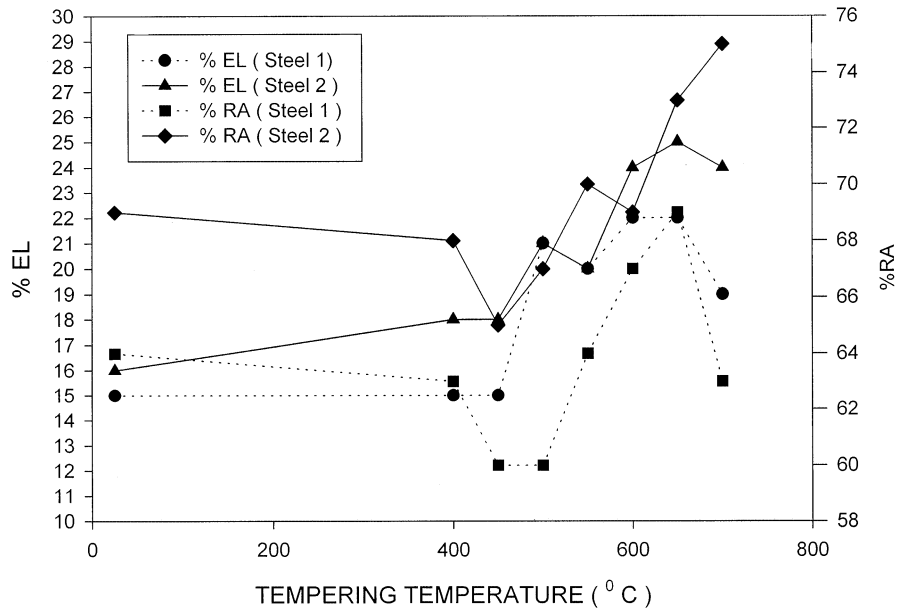

Fig. 2. Variation of elongation and reduction -in-area% of steels 1 and 2 with tempering temperature.

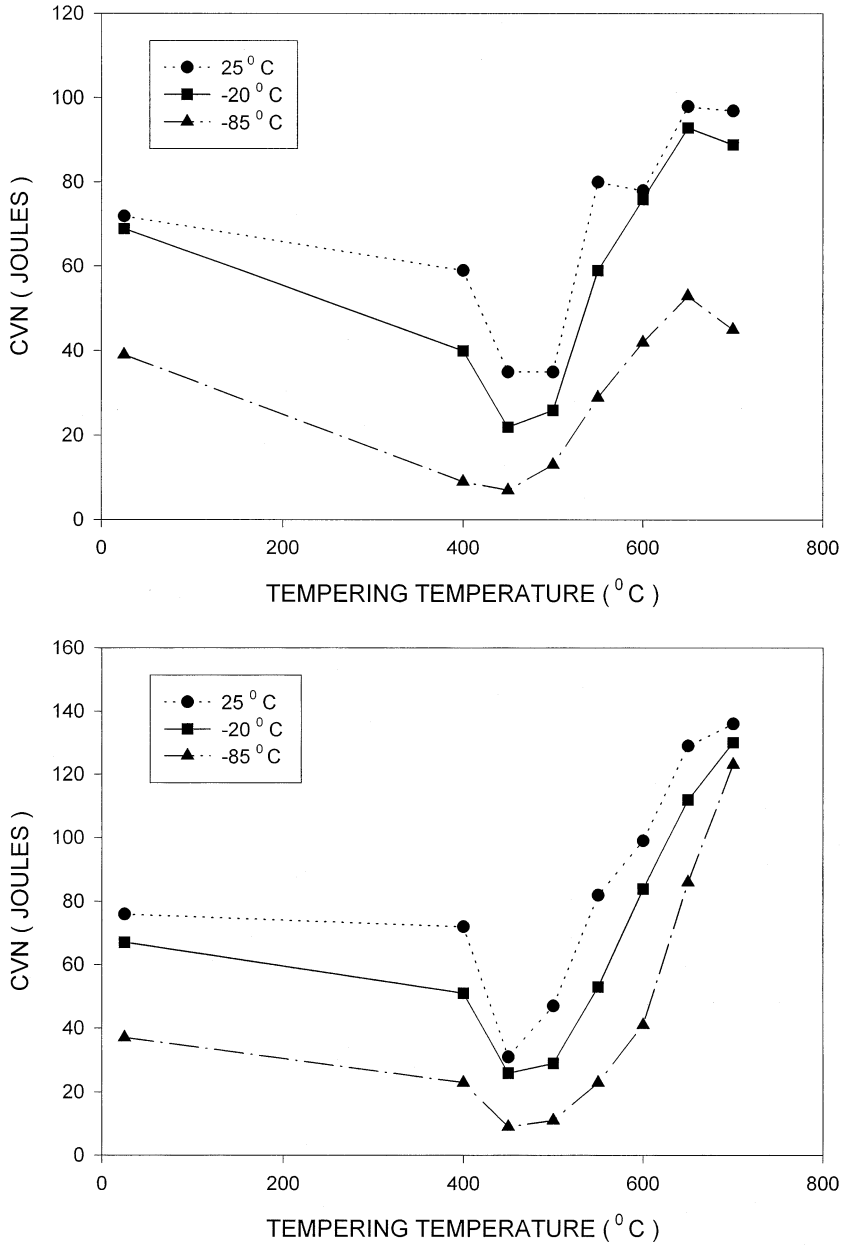

Fig. 3. (a) Variation of CVN energy of steel 1 at 25, −20 and −85°C with tempering temperature; (b) Variation of CVN energy of steel 2 at 25, −20 and −85°C with tempering temperature.

shows the BF micrograph of partially recovered martensite laths observed in steel 2. A new dark phase was found to appear at the lath boundaries which was identified by diffraction analysis to be martensite, freshly formed from intercritical austenite. The Cu precipitates were observed to have coarsened to a maximum size of 50 nm and appeared slightly elongated at this temperature. The BF and DF micrographs shown in Fig. 8 (b–c) clearly indicated the presence of numerous Cu precipitates.

Transmission electron microscopy of the steels tempered at 700°C exhibited partially recovered lath martensite (Fig. 9a) with coarse and elongated rod-shaped (maximum length: 80 nm) Cu precipitates. The volume fraction of the freshly formed martensite appeared to be more at this temperature, as can be seen from Fig. 9(b).

3.3. Fractography

Typical SEM fractographs of broken Charpy specimens tested at −85°C of as-quenched as well as tempered (at 500 and 650°C) plates of steel 2 are shown in Fig. 10 (a–c). Whereas the fracture topography of specimens pertaining to steel plates tempered at 650°C exhibited microvoids, the fracture surfaces of as-

quenched steel plates and plates tempered at 500°C essentially showed cleavage, which corresponded with poor notch toughness in these conditions.

3.4. X-ray diffractometry

X-ray diffraction studies of water-quenched and tempered plates did not reveal the presence of any retained austenite peak in either of the two steels.

4. Discussion

4.1. Mechanical properties

4.1.1. Hardness, YS and UTS

The hardness, YS and UTS values of water-quenched plates pertaining to steels 1 and 2 were much lower than that expected of a fully transformed martensitic structure and were also less than that obtained in the HSLA-100 steel investigated by us earlier [19]. This is clearly evident from the superimposed plots of hardness, YS and UTS shown in Fig. 11 (a–c). The lower hardness and strength of 14 mm thick plates in the presently investigated steels 1 and 2 can be attributed to

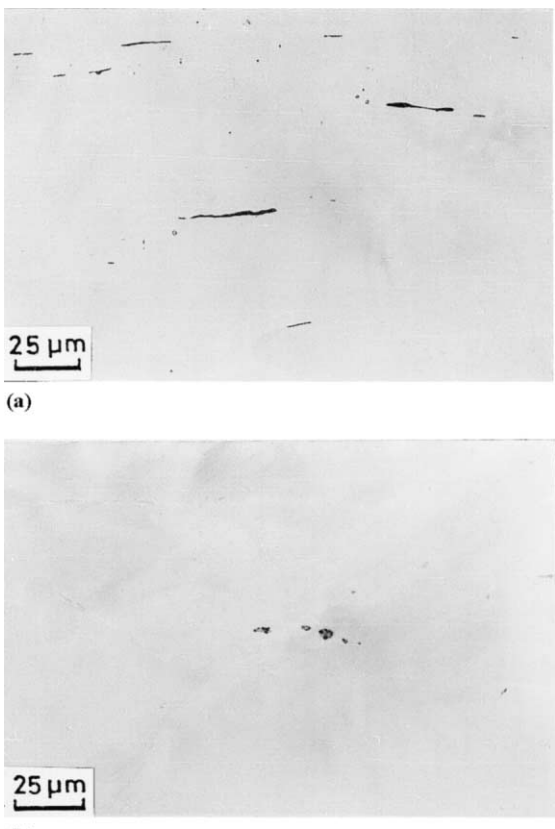

Fig. 4. Optical micrographs showing: (a) inclusion stringers in steel 1; (b) globular inclusions in steel 2.

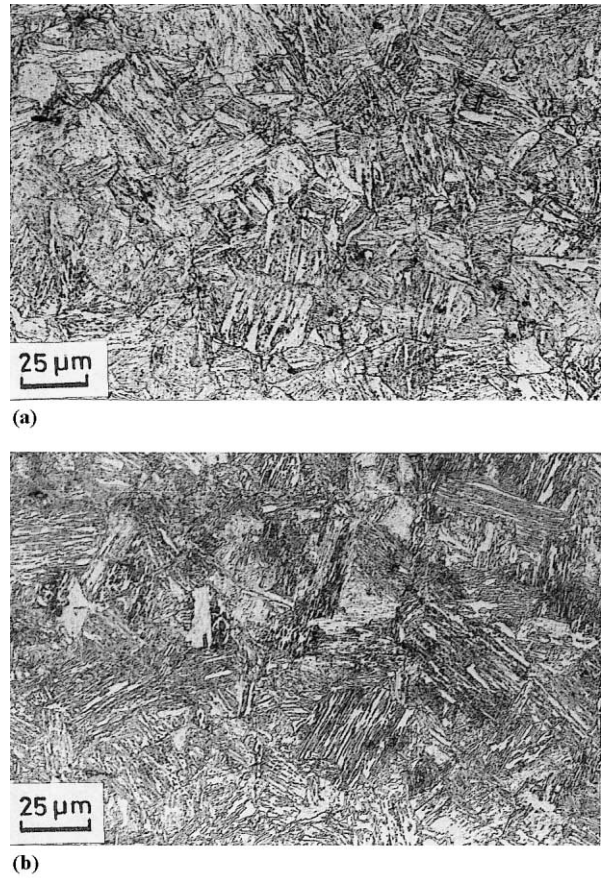

Fig. 5. Optical micrographs of steel 1 showing: (a) water quenched condition; (b) structure after tempering at 700°C.

their lower carbon contents (0.026 and 0.03 wt.%, respectively) vis-à-vis the HSLA-100 steel (C: 0.04 wt.%) investigated earlier [19]. However, the dominant reason for such behaviour seems to be the mixed microstructure of bainitic ferrite and lath martensite in steels 1 and 2 as compared to the predominantly martensitic microstructure in the earlier investigated HSLA-100 steel plates of the same section thickness.

Mujahid et al. [17] in their study on the effect of carbon content on the mechanical properties of HSLA-100 steel observed that a steel with 0.057 wt.% C yielded a hardness of 368 VHN as compared to 348 VHN in a steel with 0.036 wt.% C. The YS and UTS values were also similarly higher by 138 and 104 Mpa, respectively in the higher carbon steel. They attributed this rise in hardness and strength to enhanced martensite strengthening. Wilson et al. [4] in their studies on 0.04 and 0.06 wt.% carbon HSLA-100 steel have also observed similar strength improvement with increase in carbon content. While the YS of a 0.04 wt.% carbon steel in water-quenched condition was found to be 704 MPa, an improvement of 179 MPa was observed for the 0.06 wt.% carbon steel. According to them, the predominantly martensitic structure in the 0.06 wt.%

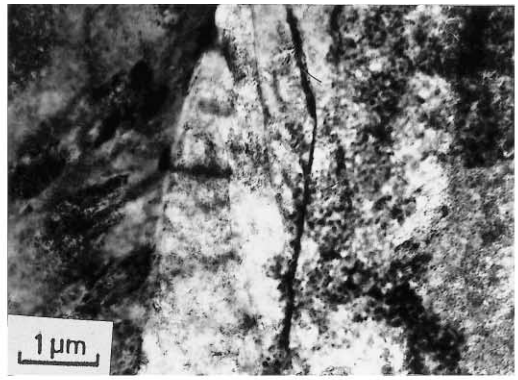

(a)

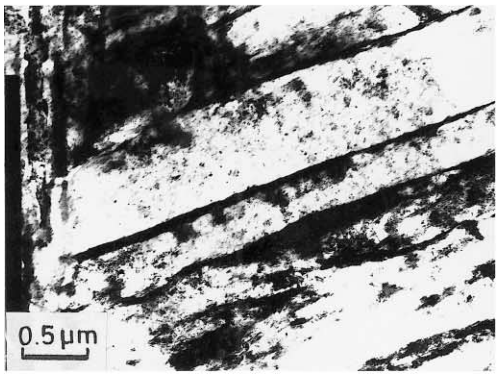

(b)

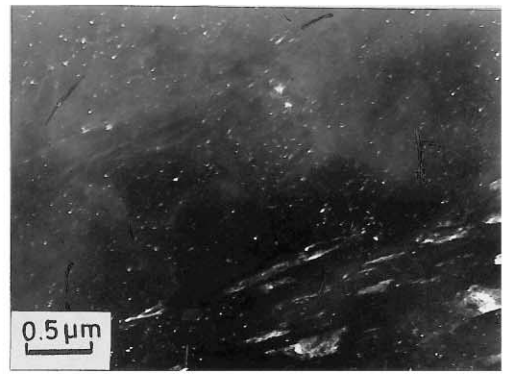

(c)

(d)

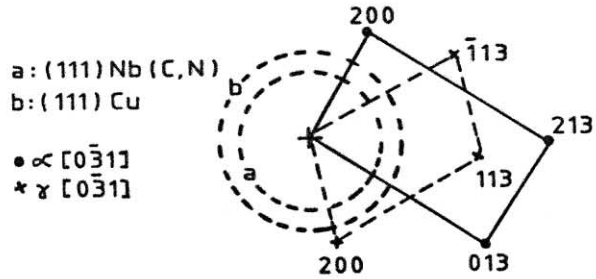

(e)

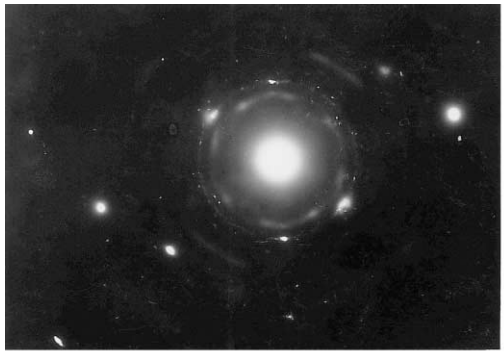

(f)

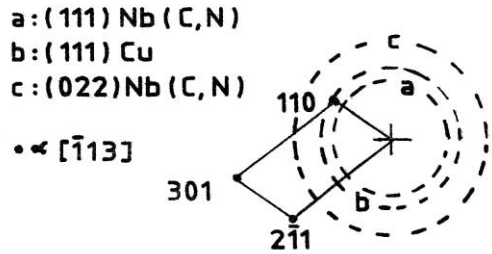

(g)

Fig. 6. Transmission electron micrographs of steel 1 in water-quenched condition: (a) BF image showing predominantly bainitic ferrite; (b) BF image; and (c) DF image showing predominantly martensitic region with retained austenite at lath boundaries and precipitates; (d) SAD pattern; and (e) index of SAD pattern identifying retained austenite; (f) SAD pattern of precipitates; and (g) index of SAD pattern identifying precipitates of Nb(C,N) and Cu.

carbon steel as compared to the mixed bainite–martensite microstructure present in the 0.04 wt.% carbon steel, was responsible for the difference in strength levels. They further reported that at these low levels of carbon, a small increase in carbon content could induce a large effect on the hardenability of HSLA-100 steel. The present study supports this conclusion.

During tempering in the range of 25–500°C, the hardness, YS and UTS of steels 1 and 2 were found to increase and reached maximum values (Fig. 1) after tempering at 500°C. The profuse precipitation of Cu at 500°C contributed towards significant increase in the strength and hardness by pinning the dislocations and restricting their movements. Similar rise in hardness and strength were also observed by earlier researchers at this stage of tempering [15,17]. Mujahid et al. [17] and Fox et al. [15] have both attributed this rise in strength to the formation of coherent Cu precipitates at this tempering temperature. Similar to the views of earlier workers [20,21], Fox et al. [15] had also considered the possible role of incoherent Cu precipitates towards strength increment which is in agreement with the present work. Incidentally, the hardness, YS and UTS of the HSLA-100 steel investigated by us earlier had registered similar rise at this temperature [19].

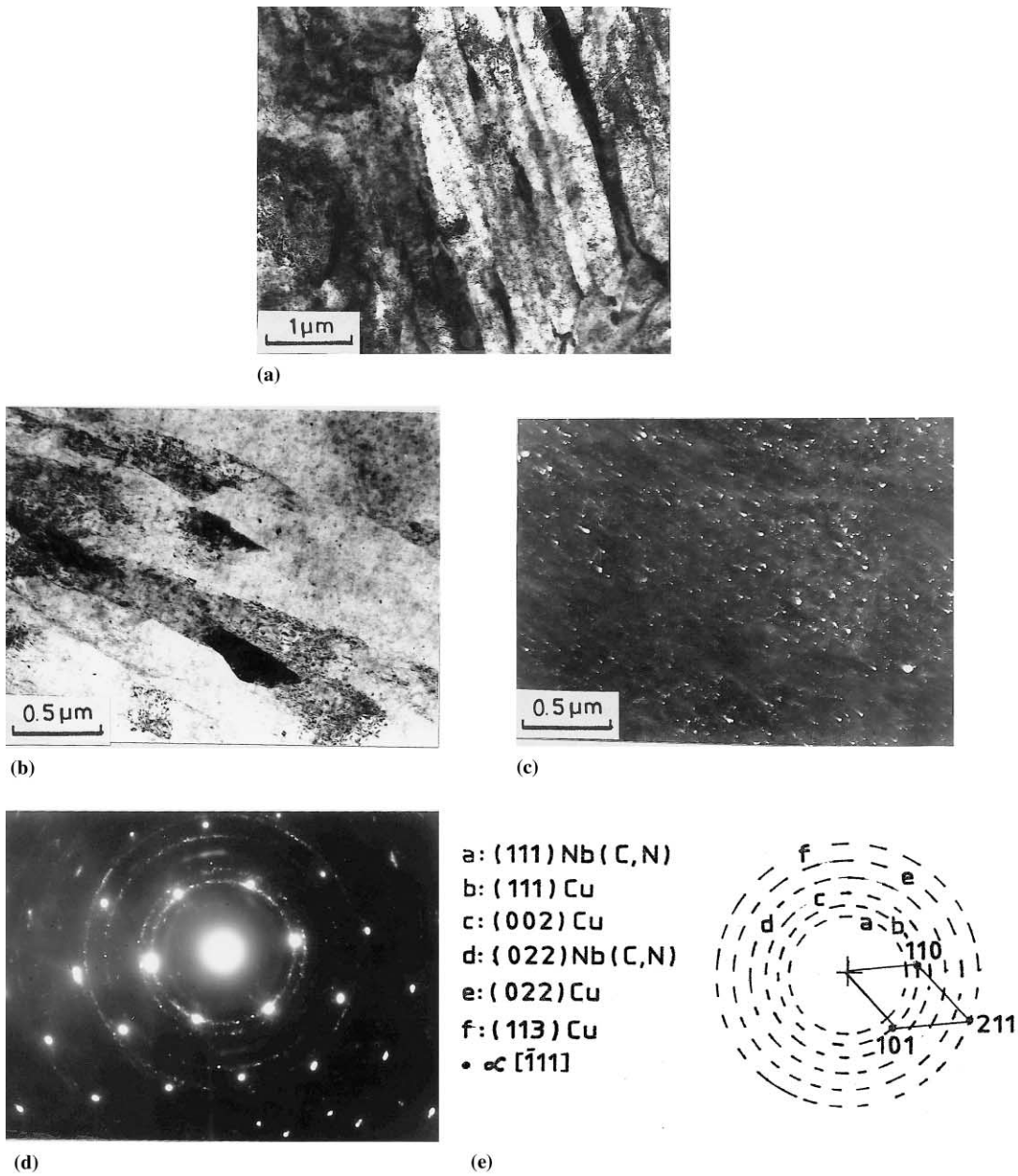

Fig. 7. Transmission electron micrographs of steel 1 tempered at 500°C: (a) BF image depicting unrecovered martensite laths in a martensite region; (b) BF image; and (c) DF image showing profuse precipitation of Cu throughout the matrix; (d) SAD pattern; and (e) index of SAD pattern identifying Cu and Nb(C,N) precipitates.

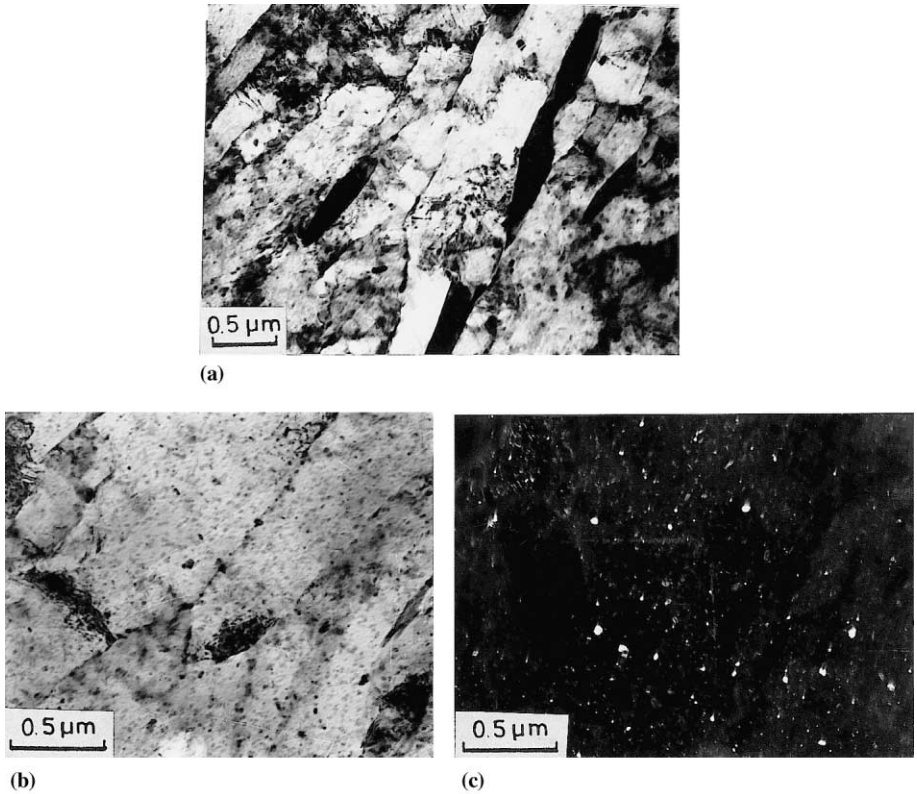

Fig. 8. Transmission electron micrographs of steel 2 tempered at 650°C showing: (a) partially recovered matrix with new dark phase at martensite lath boundaries; (b) BF; and (c) DF image of coarsened Cu precipitates.

On tempering in the range of 500–650°C, continuous decrease in hardness, YS and UTS occurred in both the steels owing to recovery of the lath martensite structure and the coarsening of Cu precipitates which allowed increased dislocation movements (Fig. 8 b and c). Earlier researchers [15,17] had also observed a similar fall in hardness and strength of HSLA-100 steel in this temperature range. They attributed this phenomenon to the loss of coherency and coarsening of Cu precipitates. The HSLA-100 steel investigated by us earlier had also exhibited a similar reduction in hardness and UTS in this temperature range as can be seen from the superimposed plots shown in Fig. 11 (a, c).

At tempering temperatures above 650°C, the hardness, YS and UTS of steels 1 and 2 were found to decrease further in contrast to the HSLA-100 steel [19], where a small rise in hardness and UTS was observed (Fig. 11 a–c). The marginal rise in hardness and UTS of the HSLA-100 steel was due to the incidence of a higher content of freshly formed martensite from intercritical austenite. Being low in carbon content, steels 1 and 2 are expected to possess lower hardenability and hence result in lesser formation of fresh martensite from intercritical austenite. Thus the influence of freshly formed martensite in steels 1 and 2 is rather insignificant in registering an increase in hardness and UTS in this temperature range.

4.1.2. Elongation and % reduction-in-area

The elongation values of steels 1 and 2 remained more or less same (15 and 18%, respectively) upto 450°C and showed marginal improvement upon tempering in the range of 500–700°C. The elongation values significantly improved after tempering at 650°C, attaining maximum values of 22 and 25% for steels 1 and 2, respectively.

For water-quenched and tempered steels, the % RA of steels 1 and 2 decreased upon tempering at 450°C, and improved during tempering in the range of 500–700°C. In case of steel 1, the maximum % RA was achieved at 650°C tempering temperature, whereas in case of steel 2, the maximum value was achieved at 700°C.

The lowering of elongation and reduction-in-area values after 450°C tempering can be attributed to over strengthening of the matrix by profuse Cu precipitation, whereas, matrix softening at higher tempering temperatures (500–700°C) was instrumental in achieving higher % EL and RA values. This behaviour is in agreement with the results of other researchers [12,17] as well as the author's earlier work on HSLA-100 steel [19].

4.1.3. Charpy impact toughness

The Charpy impact toughness values of as-quenched plates of steels 1 and 2 were very good even at −85°C. This, however, decreased considerably upon tempering near 500°C, which incidentally coincided with the peak hardening temperature associated with profuse precipitation of copper. The HSLA-100 steel investigated by us earlier [19] also showed a substantial drop in CVN impact energy (Fig. 11d) after 450°C tempering. It is expedient to mention that earlier researchers [4,12,17] had also reported similar drop in CVN energy in this tempering temperature range.

The continuous enhancement in CVN energy for steels 1 and 2 upon tempering beyond 500°C (peak values obtained at 650 and 700°C tempering, respectively) can be attributed to partially recovered lath martensite matrix and coarsening of Cu precipitates that could arrest the propagation of cleavage cracks. The increase in % EL and RA values at this stage, as discussed earlier, matched the rise in CVN impact energy. Although the significant improvement in CVN energy upon tempering near 650°C has been attributed to the formation of highly alloyed, thermally stable austenite at lath boundaries by Mujahid et al. [16,17], only traces of retained austenite at lath boundaries were detected in our present study in the as-quenched steels which might continue to exist in tempered conditions as well. The detection of retained austenite through X-ray diffraction was not possible in this study owing to its extremely low content. Hence, the explanation offered by earlier investigators on the presence of retained austenite and its influence on impact toughness is not convincing.

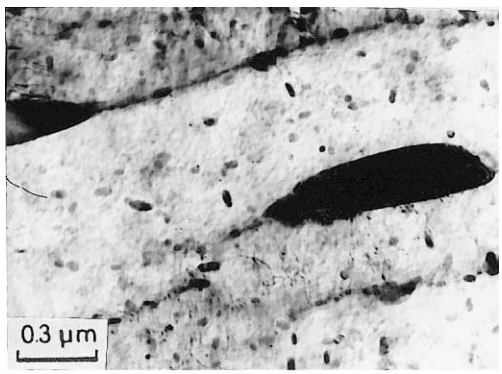

(a)

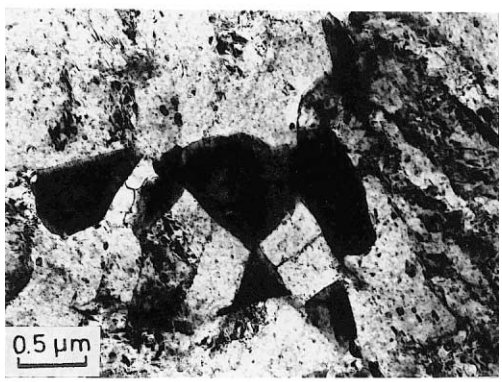

(b)

Fig. 9. Transmission electron micrographs of steel 2 tempered at 700°C showing: (a) partially recovered matrix with elongated Cu precipitates; (b) more dark phase at martensite lath boundaries.

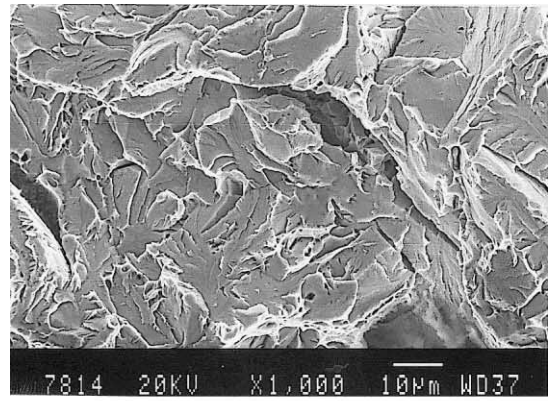

(a)

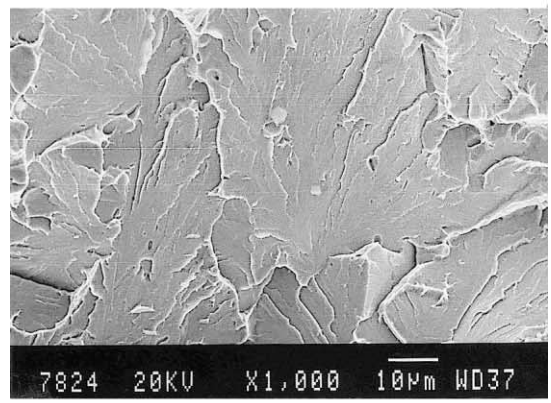

(b)

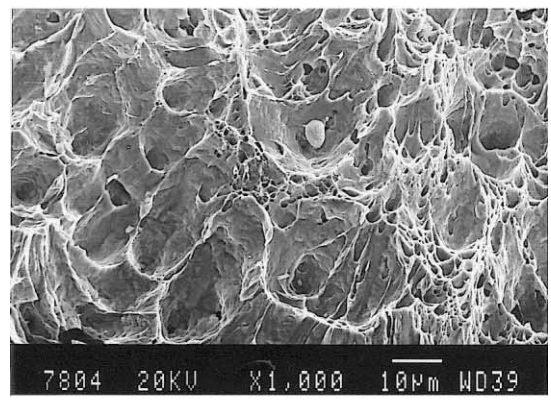

(c)

Fig. 10. SEM fractographs of Charpy impact tested sample of steel 2 at −85°C showing: (a) cleavage facets in as-quenched condition; (b) cleavage facets after 500°C tempering; (c) microvoids after 650°C tempering.

Comparing the CVN energies of steels 1 and 2 with that of the HSLA-100 steel investigated earlier [19], it was found that CVN energy of steel 1 was lowest at all conditions and test temperatures. The elongated silicate and sulphide inclusions found in steel 1 (Fig. 1a) are considered to be responsible for its lower CVN energy as compared to steel 2 where inclusions (Fig. 1b) were mostly globular and their volume percent (Table 2) was lower. The CVN energy of the HSLA-100 steel studied earlier was however, higher than that of steels 1 and 2 owing to slightly higher carbon content (~ 0.04 wt.%) in the former steel than that (0.026–0.03wt.%) in the latter steels. Earlier researchers [4,17] had shown that in this lower carbon level, a small increase in carbon content could have favourable effect in enhancing the CVN energy of the steel through increase in amount of martensite and decrease in the ferrite volume percent.

It is thus obvious that martensite, tempered or untempered, is better from toughness point of view as compared to a mixture of tempered martensite and bainitic ferrite which is usually observed in lower carbon HSLA-100 steels similar to those presently studied.

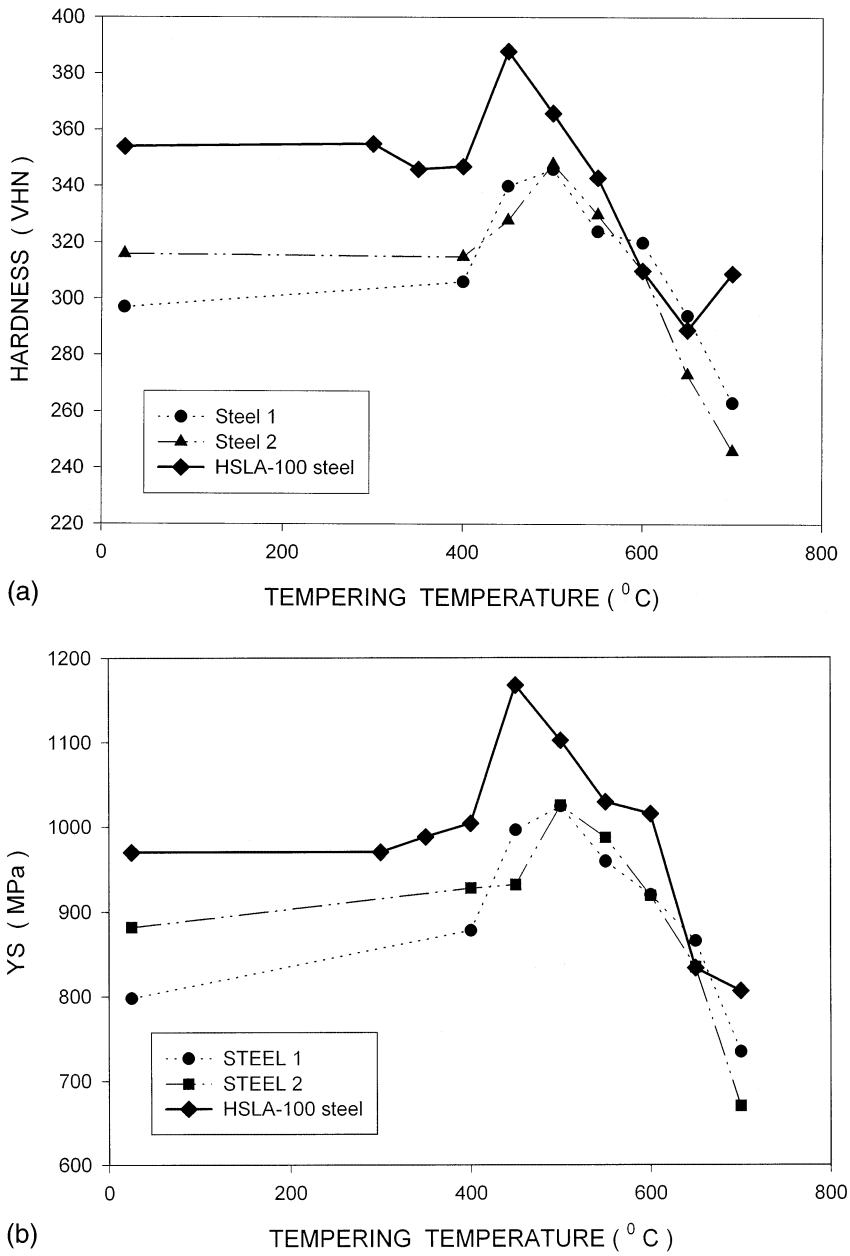

Fig. 11. Superimposed plots depicting variation of: (a) hardness; (b) YS; (c) UTS; and (d) CVN energy with tempering temperature of steels 1 and 2 along with data of author's earlier work on HSLA-100 steel.

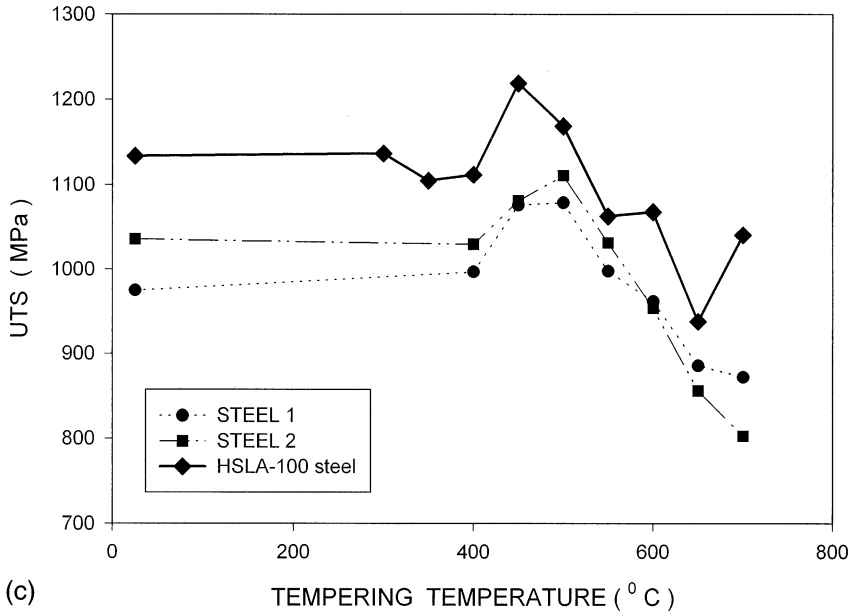

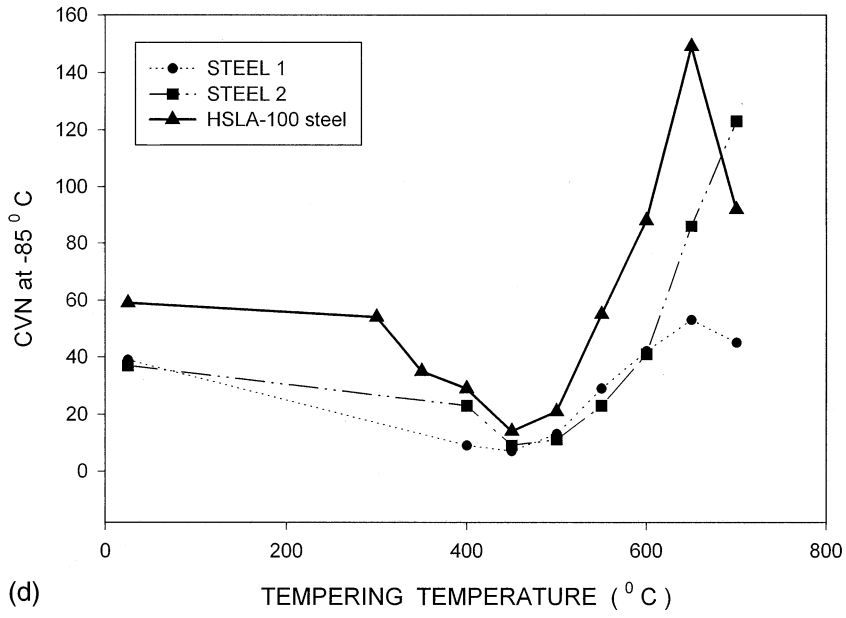

Fig. 11. (*Continued*)

4.2. Microstructure

4.2.1. As-quenched steels

In water-quenched condition, both steels 1 and 2 revealed a mixed microstructure of lath martensite and bainitic ferrite (Fig. 6 a–b). This indicates that an alloy content of upto 7 wt.% was not adequate to develop sufficient hardenability for producing a fully martensitic microstructure in 14 mm thick plates containing 0.025–0.03wt.% C. Fox et al. [15] in their studies on HSLA-100 steel plates of 19 and 31 mm section thickness and carbon content in the level of 0.048 wt.% had also observed the existence of bainitic ferrite along with martensite in water quenched condition. Wilson et al. [4] in their studies on 51 mm thick plates of HSLA-100 steel reported that whereas the microstructure in a 0.06 wt.% C steel was martensitic, it was bainitic in 0.04 wt.% C steels. Although the incidence of low volume fractions of retained austenite at lath boundaries of quenched HSLA-100 steel was reported by many researchers, this was not supported by diffraction. Practically, it was very difficult to obtain a SAD pattern for retained austenite in the quenched steel since its volume fraction was very small and appeared (Fig. 6c) in traces at lath boundaries. The approximate M_S temperature for HSLA-100 steel is 450°C and hence the probability of austenite to be retained at room temperature is very low.

The existence of Nb(C,N) precipitates in the quenched structure is not unexpected because these might have formed during the hot-rolling process and would not have gone into solution at the austenitising temperature of 950°C. Although the precipitation of Nb(C,N) during hot-rolling of HSLA steel was reported earlier [22], the occurrence of Cu precipitates in the quenched steel, as observed in the present investigation, was unusual and not reported by previous workers. This has possibly occurred as a result of higher copper content ($\sim$ 1.73 and 1.52 wt.% in steels 1 and 2, respectively) in the present steels causing partial segregation of Cu.

4.2.2. Tempered steels

The steels tempered at 500°C showed profuse Cu precipitation in the supersaturated α matrix along with the pre-existing Nb(C,N) precipitates. The Cu precipitates did not coarsen much as compared to that in as-quenched steel (Fig. 7c). Mujahid et al. [17] observed the presence of fine copper clusters manifested by Moire patterns when the steel was tempered at 450°C. Spherical Nb (C,N) precipitates of diameter ranging between 10 and 30 nm were also observed by them and the present work confirms these findings. Few attempts were made in the past to reveal the coherent nature of these copper precipitates in peak-aged condition. Earlier workers like Hornbogen et al. [23], Osamura et al. [24] and Pande et al. [25] in their study of Fe–Cu alloys clearly indicated that bcc copper rich clusters precipitated first from supersaturated α-iron, which subsequently transformed to fcc phase when they grew beyond a critical size. None of the earlier investigators, however, observed bcc Cu clusters by transmission electron microscopy. While Osamura et al. [24] and Pande et al. [25] used small angle neutron scattering method of characterization of the coherent Cu precipitates which had bcc structure in their early stage of nucleation and precipitation, Goodman et al. using field-ion-microscopy observed particles (10–12 Å size) of a highly supersaturated Fe–Cu solid solution formed after ageing for 1 h at 500°C. Owing to the complexity of the alloy system and the presence of large numbers of dislocations and other precipitates in the tempered steels, it was not possible to opine on the coherent nature of the copper precipitates in the present study.

The steels tempered at 650°C showed Cu precipitates in partially recovered lath martensite matrix (Fig. 7b); the precipitates were found to be coarse and slightly elongated as shown in Fig. 8(b, c). A new dark phase, that has been established to be martensite (by diffraction analysis), could be observed (Fig. 8a) along the laths in small amounts. Although some earlier workers [14,17] had presumed this phase to be austenite, newly formed at intercritical temperature and retained at room temperature owing to its rich alloy content, there was no adequate diffraction evidence to corroborate this effect.

Steels tempered at 700°C exhibited greater volume fraction of this new dark phase (martensite) in partially recovered matrix. This is expected since the temperature range was above AC_1 and hence form more amount austenite which would subsequently get transformed to fresh martensite (Fig. 9a–b) on cooling. The Cu precipitates (Fig. 9a) were found to have coarsened and elongated substantially to become rod shaped.

Thus in summary, it can be mentioned that the mixed microstructure of bainitic ferrite and martensite in quenched steels 1 and 2 led to lower hardness and strength compared to the predominantly martensitic microstructure of the HSLA-100 steel studied earlier [19]. In addition to lower C content, higher inclusion volume fraction and the incidence of elongated silicate and sulphide inclusion stringers (particularly in steel 1), resulted in lower impact toughness of these steels compared to the HSLA-100 steel investigated earlier [19]. On tempering, profuse precipitation of Cu occurred in steels 1 and 2 in the range of 450–500°C leading to the attainment of peak hardness and the accompanying loss of toughness. In the temperature range between 650 and 700°C, partial recovery of the matrix and the coarsening of Cu precipitates led to considerable enhancement of impact toughness with deterioration of hardness and strength. The retained austenite content however, was found to be very small in quenched condition and indicated that it virtually did not affect the mechanical properties of quenched and tempered HSLA-100 steels. Similarly, the Nb(C,N) precipitates commonly observed in both as-quenched and tempered conditions, were not expected to exert any significant influence on the tempering behaviour of the steels.

5. Conclusions

(1) In water-quenched condition, the steels exhibited a mixed microstructure of martensite and bainitic ferrite with traces of retained austenite at martensite lath boundaries. Incidence of Cu precipitates along with Nb(C,N) particles could be observed in the matrix of the as-quenched steels. At 500°C tempering temperature, a large number of fine Cu precipitates were found in the matrix, while partial recovery of the matrix and coarsening of Cu precipitates occurred on tempering at or above 650°C.

(2) The hardness, YS and UTS attained peak values (347 VHN, 1024 MPa, 1079 MPa for steel 1 and 347 VHN, 1025 MPa and 1111 MPa for steel 2) after tempering at 500°C. Thereafter, the hardness and strength values dropped continuously, reaching minimum at 700°C. The hardness and strength of the present steels were slightly lower than that of the

HSLA-100 steels investigated earlier [19]. In the steels investigated, this was possibly due to their lower carbon contents (0.02–0.03wt.%) which resulted in lower hardenabilities and more amount of bainitic ferrite in the structure.

The Charpy impact toughness values of both the steels were lower in the 450–500°C range of tempering temperature. Beyond this, there was a gradual improvement in toughness, reaching maximum values of 53 and 123 J at −85°C for steels 1 (tempered at 650°C) and 2 (tempered at 700°C), respectively. Higher volume fraction and elongated morphology of non-metallic inclusions in air- melted steel (steel 1) was found to be primarily responsible for its lower CVN energy value. The CVN energy of both steels 1 and 2 were lower than the earlier investigated HSLA-100 steels [19] owing to both higher NMI content and lower hardenability i.e. presence of more acicular ferrite.

Acknowledgements

The authors thank the management of the R&D Centre for Iron and steel, Steel Authority of India Limited, Ranchi and the Head of the department of Metallurgical Engineering, Banaras Hindu University, Varanasi, India for providing necessary experimental facilities and encouragement in pursuing this work.

References

[1] B.A. Graville, Proceedings on the International Conference on Welding of HSLA (microalloyed) structural Steels, ASM International, Metals Park, Ohio, USA, 1978, p. 85.
[2] E.J. Czyryca, Key Engineering Materials, vols. 84–85, Transtech Publications, Switzerland, 1993, p. 491.
[3] M.R. Krishnadev, Proceedings on the International Conference on HSLA Steels: Technology and Applications, ASM International, Metals Park, Ohio, USA, 1984, p. 77.
[4] A.D. Wilson, E.G. Hamburg, D.J. Colvin, S.W. Thompson, G. Krauss, Proceedings on the International Conference on Microalloyed HSLA Steel, Microalloying'88, ASM International, Metals Park, Ohio, USA, 1988, p. 259.
[5] R.H. Philips, J.G. Williams, J.E. Croll, Proceedings on the International Conference on Microalloyed HSLA Steels, Microalloying, ASM Interrnational, Metals Park, Ohio, USA, 1988, p. 235.
[6] M.T. Miglin, J.P. Hirth, A.R. Rosenfield, W.A.T. Clark, Metall. Trans. 17A (1986) 791.
[7] S.S. Banadkouki Ghasemi, D. Yu, D.P. Dunne, ISIJ Int. 36 (1996) 61.
[8] G.E Hicho, C.H. Brady, L.C. Smith, R.J. Fields, J. Heat Treating 5 (1987) 7.
[9] G.E. Hicho, S. Singhal, L.C. Smith, R.J. Fields, Proceedings on the International Conference on HSLA Steels, Technology and Applications, ASM International, Metals Park, Ohio, USA, 1984, p. 705.
[10] Abe Takashi, Kurihara Masayoshi, Tagawa Histoshi, Trans. ISIJ 27 (1987) 478.
[11] A.D. Wilson, J. Metals 29 (1987) 39.
[12] S.J. Mikalac, M.G. Vassilaros, Proceedings on the International Conference on Processing, Microstructure and Properties of Microalloyed and other Modern HSLA Steels, ISS, Warrendale, PA, 1991, p. 331.
[13] R.P. Foley, M.E. Fine, Proceedings on International Conference on Processing, Microstructure and Properties of Microalloyed and other Modern HSLA Steels, ISS, Warrendale, PA, USA, 1991, p. 315.
[14] R.P. Foley, M.E. Fine, Speich Symposium Proceedings, ISS, Warrendale, PA, USA 1992, p. 139.
[15] A.G. Fox, S. Mikalac, M.G. Vassilaros, Speich Symposium Proceedings, ISS, Warrendale, PA, USA 1992, p. 155.
[16] M. Mujahid, A.K. Lis, C.I. Garcia, A.J. DeArdo, Key Engineering Materials, vol. 84-85, Transtech Publications, Switzerland, 1993, p. 209.
[17] M. Mujahid, A.K. Lis, C.I. Garcia, A.J. DeArdo, J. Mater. Eng. Perform. 7 (1998) 247.
[18] G.C. Hwang, S. Lee, J.Y. Yoo, W.Y. Choo, Mater. Sci. Eng. A252 (1998) 256.
[19] S.K. Dhua[1], D. Mukerjee[1], D.S. Sarma[2], [1]R&D Centre for Iron and Steel, Steel Authority of India Limited, Ranchi, India and [2]Department of Metallurgical Eng., Banaras Hindu University, Varanasi, India, Unpublished research, 2000.
[20] S.R. Goodman, S.S. Brenner, J.R. Low, Metall. Trans. A4 (1973) 2363.
[21] P.J. Othen, M.L. Jenkins, G.D.W. Smith, W.J. Phythian, Phil. Mag. Letts. 64 (1991) 383.
[22] M.A. Cooke, B.H. Chapman, S.W. Thomson, Scripta Metallurgica 26 (1992) 1553.
[23] E. Hornbogen, R.C. Glenn, Trans. AIME 218 (1960) 1064.
[24] K. Osamura, H. Okuda, S. Ochiai, M. Takashima, K. Asano, M. Furusaka, K. Kishida, F. Kurosawa, ISIJ Int. 4 (1994) 359.
[25] C.S. Pande, M.A. Imam, C.L. Vold, E. Dantsker, B.B. Rath, Key Engineering Materials, vols. 84–85, Transtech Publications, Switzerland, 1993, p. 145.